Solid Freeform Fabrication 2023: Proceedings of the 34th Annual International Solid Freeform Fabrication Symposium – An Additive Manufacturing Conference
Reviewed Paper

A comparison of mechanical properties from natural and process-induced interfaces in filament extrusion AM of polymer blends

Camden A. Chatham* and Donald W. Benza*

*Advanced Engineering Division, Savannah River National Laboratory, Aiken, SC USA
E-mail: camden02.chatham@srnl.doe.gov

Abstract

Polymer blends are commonly tuned for specific applications to achieve desired properties otherwise inaccessible or prohibitively expensive to obtain via homopolymers. The interfacial characteristics of the polymer A-polymer B interface and resultant domain sizes govern key performance properties. Micro- and meso-scale morphology forms through the interplay of surface forces between the polymers and between each polymer and the surrounding atmosphere. Analogously, the layer-layer and road-road interfaces of material extrusion (MEX) additive manufacturing (AM) govern key performance properties of printed parts. This work explores the effect of layer height on the thermomechanical performance of polystyrene (PS)-polycarbonate (PC) blends. Filament is prepared from a 50/50 weight ratio of the two polymers and compared against dual-nozzle printing where every layer alternates between PS or PC homopolymer forming a part with an overall 50/50 polymer ratio. Typical indicators of polymer blend compatibility are also studied.

Introduction

Additive manufacturing's (AM) layerwise manufacturing paradigm is commonly touted for its ability to fabricate complex geometries without shape-specific tooling. This fabrication method enables lattices to be fabricated just as easily as solid blocks leading to the summary statement that "complexity is free" in AM. However, material behavior at interfaces is significantly different from that observed in the bulk. Therefore, interfacial bonding (both interlayer and intra-layer) is a critical aspect of AM processes to understand. Interfacial strength in composite and adhesive systems are well-studied due to the regularity at which part failure occurs at the interfaces between dissimilar materials in part due to the interface being weaker than regions where bulk behavior dominates.[1] When using the fused filament fabrication (FFF) sub-technology of material extrusion (MEX) to fabricate parts from polymer blends, there exist two types of interfaces: (i) domain boundaries between constituent polymers (microscale) and (ii) process-induced boundaries between layers and roads (mesoscale). These interfaces are hierarchical for polymers blended during filament production as the domain boundaries will be substantially smaller than the typical layer thickness of 100's of microns.

Several FFF printer manufacturers have developed machines with multiple extrusion nozzles enabling multiple materials to be incorporated into a single part, including the Ultimaker S3[2] used for the present work. Although other authors have reported on the interfacial strength,[3–5] they fabricated specimens with a single dissimilar polymer layer interface. This method enables ease of measurement for interfacial strength; however, it provides no insight into whether a dual-extrusion part can approximate the properties of a polymer blend prepared in advance. To the authors' knowledge, no published work compares the mechanical performance of a traditionally

blended filament with a structure of alternating homopolymer layers comprising an analogous polymer blend ratio. Figure 1 depicts a cartoon representation of parts produced from traditionally blended filament and alternating homopolymer layers. This can be considered an expansion of nano/microlayered coextrusion[6,7] as it promotes the macro-scale exhibiting of interfacial behavior and properties relative to bulk behavior and properties by decreasing the layer size and increasing the number of interfaces. Current FFF technologies use layer heights much larger than the 10s of nanometers usually needed for geometric confinement behavior,[6] but the relative increase in volume of interphase polymer compared with bulk molding technologies is significant.

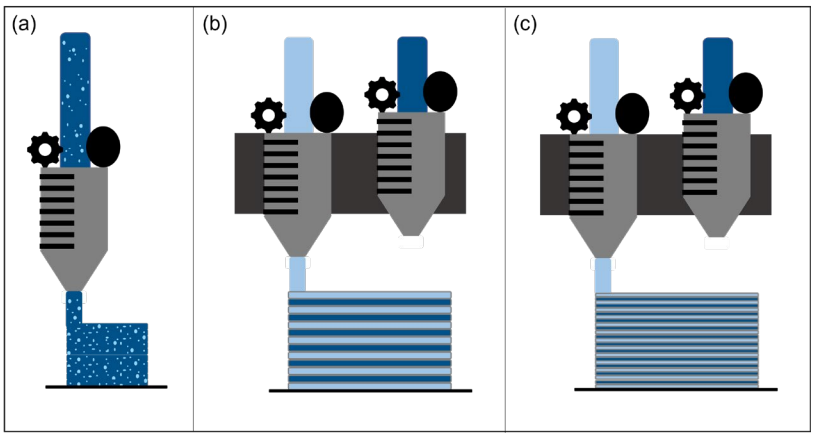

Figure 1: Cartoon depiction of a generic part made from (a) traditionally blended filament and (b) alternating homopolymer layers via FFF. Subfigure (c) depicts the alternating homopolymer layers method using thinner layers producing more interfaces.

Self-segregated domains occur in polymer blends due to chemical differences between constituent polymers. These differences are often characterized using the Interaction Parameter (χ) with miscible blends having a negative value and compatible blends having values less than 0.5.[8] The reported interaction parameter for PC and PS is 0.038 by Kim and Burns.[9] Phase diagrams describing the resulting blend morphology from various combinations of polymers are the subject of painstaking scientific work. Such work can be leveraged for tailored self-assembly into morphologies desired for specific applications. Various morphologies can be achieved for the same polymer blend ratio through altering processing conditions.

When blending two polymers, one might expect the performance behavior of the blend to be some combination of the performance from the two constituents and the newly created, third mixed phase. The study of the characteristic length scales and how those domains affect final part performance has been published by Chevallier, et al.,[10] Tanaka, et al.,[11] and Ayoub, et al.[12] They report changes in observed domain sizes with changes to composition and processing. Other researchers have found through transmission electron microscopy (TEM) that the width of the PS-PC interface is 32 nm.[13] Often phase separated behavior shows a profound effect on melt viscosity, which in turn alters solid-state mechanical properties.[11] Given the importance of these characteristic lengths of phase separation, the present work demonstrates the impact of nominally equivalent blends of polystyrene and polycarbonate by either blending the two components in a twin screw extruder prior to making filament or else extruding alternating layers of each homopolymer. Each method produces samples with distinct spatial arrangement of each blend

component. Traditionally mixed samples via twin-screw extrusion, like several of the literature-cited studies, are expected to have PS droplets dispersed inside a continuous PC phase[14] or else a co-continuous phase;[15] samples prepared from alternating layers are expected to largely retain their layered structure. The difference in response to both oscillatory shear loading and creep recovery are explored and reported for these materials.

Experimental

Materials, Filament Preparation, and FFF Printing.

Polystyrene (Sigma Aldrich) and bisphenol-A polycarbonate (3DXTECH) were sourced in pellet-form for in-house blending and filament preparation. Homopolymer filament was prepared using a Filabot EX2 filament making system. 2.5 ± 0.1 mm filament was extruded at 245 °C. A 50/50 w/w PC/PS blends were prepared using a Liestritz twin screw extruder prior to re-pelletization. Filament was prepared from the blended pellets at 245 °C using the Filabot EX2 filament extruder. All samples were fabricated using an Ultimaker S3 dual extrusion FFF machine with a bed temperature of 110 °C, nozzle temperature of 260 °C, nozzle diameter of 0.4 mm, and print speed of 10 mm s^{-1}.

Characterization

Dynamic mechanical analysis (DMA). A Mettler Toledo DMA/SDTA 1+ with shear clamping assembly was used to quantify viscoelastic properties of prepared blended polymers. Test specimen cylinders were prepared by FFF AM in the ZYX orientation (i.e., shear force applied parallel to layer interfaces). Test specimen geometries are presented in Table 1; all geometries afford a geometry factor within appropriate measurement limits according to the Mettler Toledo user manual.

The Mettler Toledo DMA/SDTA 1+ operates by switching between stress and strain controlled measurement modes. Therefore, the user sets both a force amplitude and a displacement amplitude when creating a measurement method and the oscillation cycle ends whenever *either* criterion is met (i.e., a logical "OR"). The authors report both amplitudes for completeness as "XX N force amplitude or YY μm displacement amplitude" to emphasize the logical "OR" nature of the method.

Table 1: Designed dimensions of FFF printed samples.

Layer Height [mm]	Number of Layers	Thickness [mm]	Diameter [mm]	Geometry Factor [m−1]
0.30	16	4.8	15	13.581
0.15	16	2.4	10	15.279

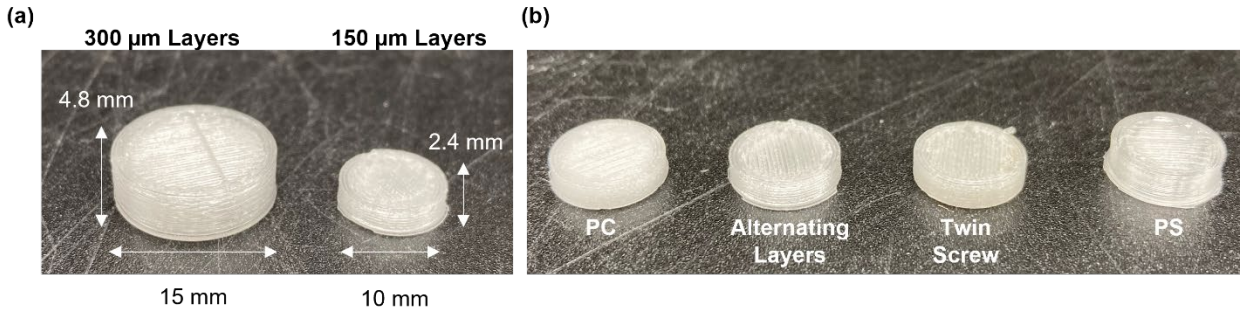

Figure 2. Photographs depicting printed shear DMA samples. (a) Comparison between the differently sized samples to account for changing layer height at constant number of interfaces. (b) Comparison of 150 µm layer height samples among the four materials tested.

An amplitude sweep was conducted at room temperature between 0.01 and 1.0 mm to determine the linear viscoelastic region. Specimens were first evaluated at room temperature by frequency sweep between 0.01 and 100 Hz at an amplitude of 2 μm before being heated at 3 °C min^{-1} at 1 Hz and 2 μm mm to 220 °C. Additionally, samples were tested for their creep response by applying a 30 N force offset for 6 h then resetting the offset to 0 N for 8 h. Creep recovery was evaluated at both 128 °C and 30 °C.

Differential Scanning Calorimetry (DSC). A Mettler Toledo DSC 3+ was used to evaluate the thermal transitions of filament made in-house. Samples were heated at 10 °C min^{-1} between 0 °C and 250 °C for two heating and cooling cycles before being heated at 20 °C min^{-1} for a final heating cycle. Initial heating cycles were used to erase any thermal memory from the sample and the final heating cycle was used to determine T_g. The midpoint method was used for determination of glass transition temperature.

Results and Discussion

Impact on the glass transition

Figure 3 reports glass transition temperature obtained by both DSC and DMA. It is typical for T_g measured via DMA (via peak of the tan(δ) curve) to be approximately 10 °C above the value obtained via DSC (midpoint of the heat flow baseline shift). The data collected from the PS and PC homopolymers follow the expected trend.

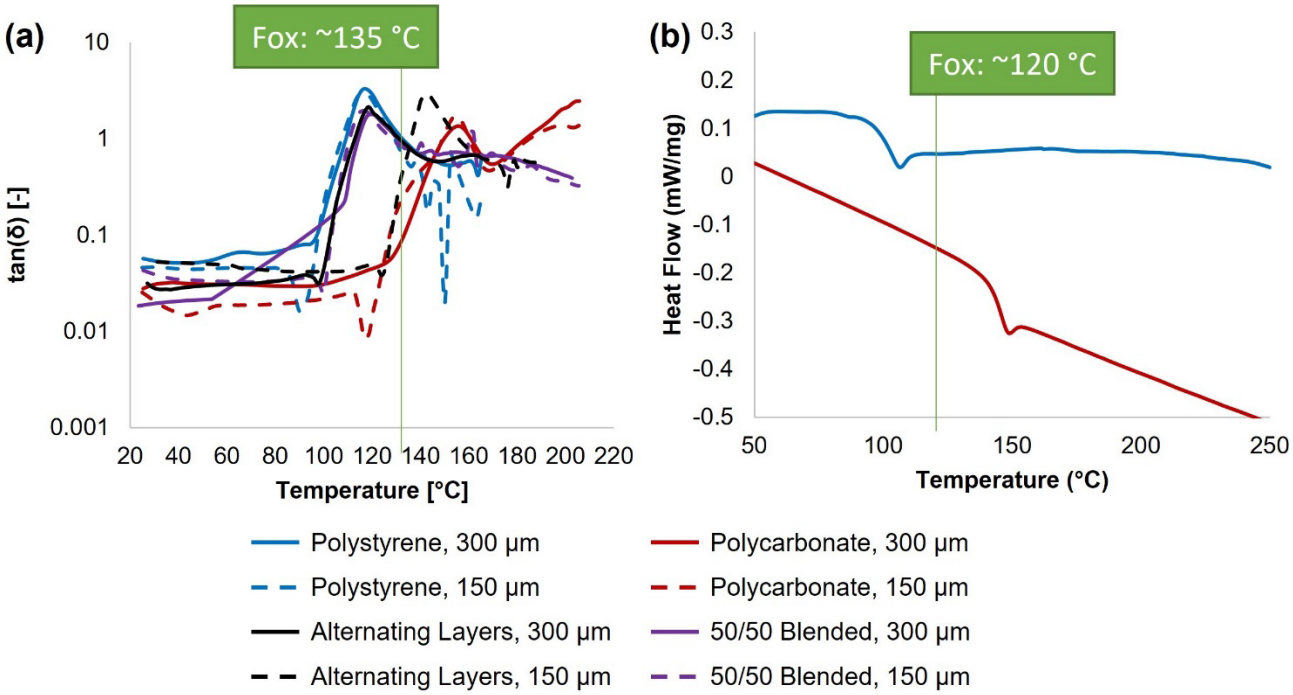

Figure 3: (a) tan(δ) versus temperature for printed homopolymers and blends. (b) Second heat of DSC depicting T_g and melt behavior for homopolymer filament.

$$\frac{1}{T_{g,blend}} = \frac{\omega_a}{T_{g,a}} + \frac{\omega_b}{T_{g,b}} \tag{1}$$

The Fox equation (Eq 1) states that the expected T_g for a miscible polymer blend is the sum of the weighted inverse temperatures of the component homopolymers. In Equation 1, the *a* and *b* designators indicate the two homopolymers present in the blend; ω is the weight fraction of that component. The unit of temperature must be Kelvin for proper usage. The expected values calculated for the studied system are 120 °C and 135 °C as measured by DSC and DMA, respectively. Although the PS-PC blends show glass transition temperatures shifted towards the

Fox predicted temperature, no blend studied should be considered "miscible." Measurements by DMA generally show the printed samples dominated by the PS T_g with, perhaps, a slight peak close to the higher temperature PC T_g. It is interesting that the alternating homopolymer layer samples printed with 150 μm layers shows a tan(δ) peak shifted above the Fox-predicted temperature and appears simply more dominated by the PC homopolymer layers than either the 300 μm alternating layer sample or either sample printed from twin screw blended filament.

Measurements by DSC in Figure 3(b) show two distinct glass transition temperatures. The extent of shift in the low and high temperature glass transition behaviors measured becomes greater with decreasing layer height. This is the hoped-for trend; printing with thinner layers affects a more homogenized blend, or at least spatially distributed morphology. Additionally, it is observed that the temperatures of the twin-screw prepared filament are shifted closer to the Fox-predicted temperature than those from the alternating homopolymer samples at equivalent layer height.

Impact on Small Amplitude Oscillatory Properties

Small amplitude oscillatory mechanical testing is often used to probe material properties without the sensitivity to surface defects that effects failure properties. Figure 4 depicts storage modulus as a function of temperature for all samples tested with the 300 μm layer height samples shown in sub-figure a and the 150 μm layer height samples in sub-figure b.

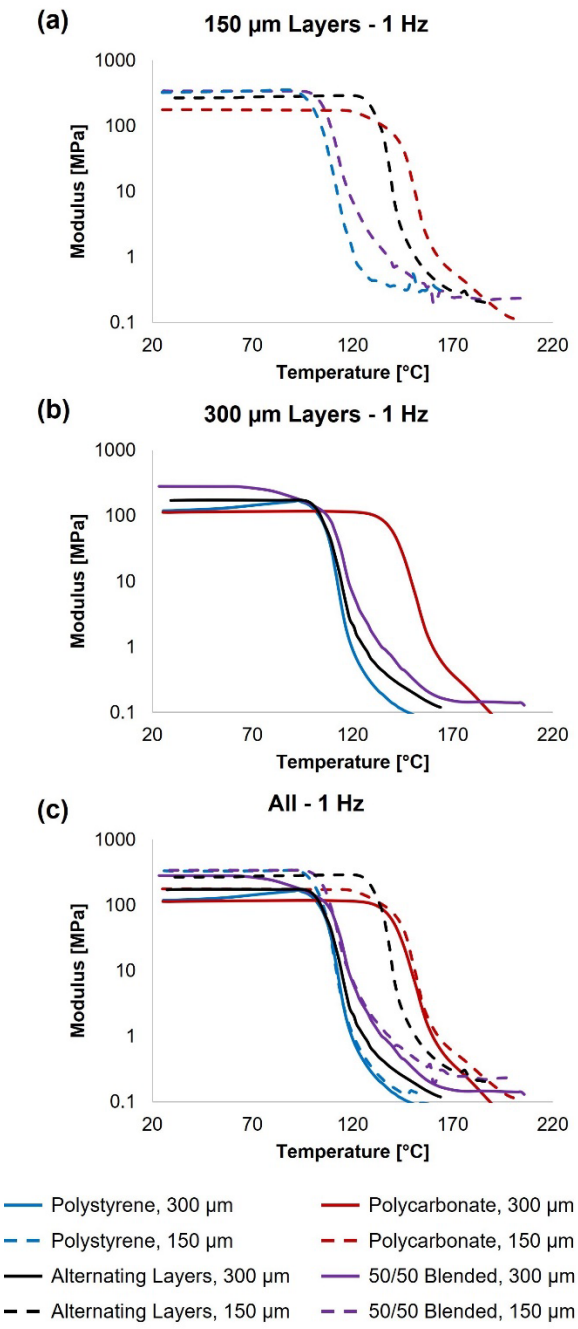

Figure 4: Comparison of storage modulus from printed homopolymers and blends with layer heights of (a) 300 μm and (b) 150 μm. DMA measured in shear mode at 1 Hz; 30 N force amplitude or 2 μm displacement amplitude.

Distinguishing behavior between PS (blue) and PC (red) homopolymers are easily observed at both layer heights. The onset of modulus decay, which can be thought of as related to heat deflection temperature, is close to 110 °C for PS but close to 160 °C for PC. Samples printed from 50/50 blended filament (purple) show onset of modulus decay alongside PS,

but the rate of decay is not as severe as the PS homopolymer. The 50/50 blended sample displays a portion of higher temperature stability and stiffness arising from the PC domains. Similar behavior is observed for the alternating layers sample at 300 μm layer height (Figure 4a; black); however, the alternating layer sample fabricated at 150 μm layer height (Figure 4b; black) shows extended temperature stability more closely resembling PC. Additionally, the samples with thinner layers show a higher modulus indicative of better interlayer adhesion. This is similar to what Frunzaverde, et al. reported in literature for ultimate tensile properties as a function of layer height.[16]

The authors hypothesize the changes in modulus are a direct result of increased polymer chain mobility at the interface. Abbott, et al. has shown the effect of layer height on temperature profile.[17] They report increased time above T_g for thinner layers given similar print conditions. Increased time at temperature (through thinner layers) has a more profound effect on the alternating layer samples, than on those pre-blended at the filament making stage. The interfacial tension at the dissimilar interface can act as an additional driving force for polymer re-entanglement beyond what is typically experienced during homopolymer printing.

Impact on Creep Recovery

Figure 5 compares the difference in creep recovery between the samples printed with alternating homopolymer layers and the samples made from 50/50 blended filament at 150 μm and 300 μm layer heights. The data in sub-figure (a) were collected at 128 °C, which is between the tan(δ) peaks measured by DMA and shown in Figure 3. After deformation at elevated temperature, the specimens printed at larger layer height recovered initial dimensions faster and more completely than the 150 μm layer height samples. The samples printed at 300 μm with twin screw blended filament were observed to have the fastest and most complete creep recovery, yet the samples printed at 150 μm with twin screw blended filament were observed to have the slowest and least complete creep recovery. This is consistent for all three load/unload cycles. Since this test was conducted above the T_g of PS and below the T_g of PC, one can expect more permanent deformation of the PS regions due to being highly mobile above T_g. The concentration of PS- and PC-rich regions in the samples with alternating layers likely affords the more consistent behavior regardless of layer height; however, the meso-scale blend morphology introduced at layer interfaces clearly affects the creep recovery of the 50/50 blended samples. The reduction in creep recovery within the time of observation with decreasing layer height (i.e., increased number of interfaces per unit length) implies that the PS plays a major role in the interfacial behavior of the blended samples.

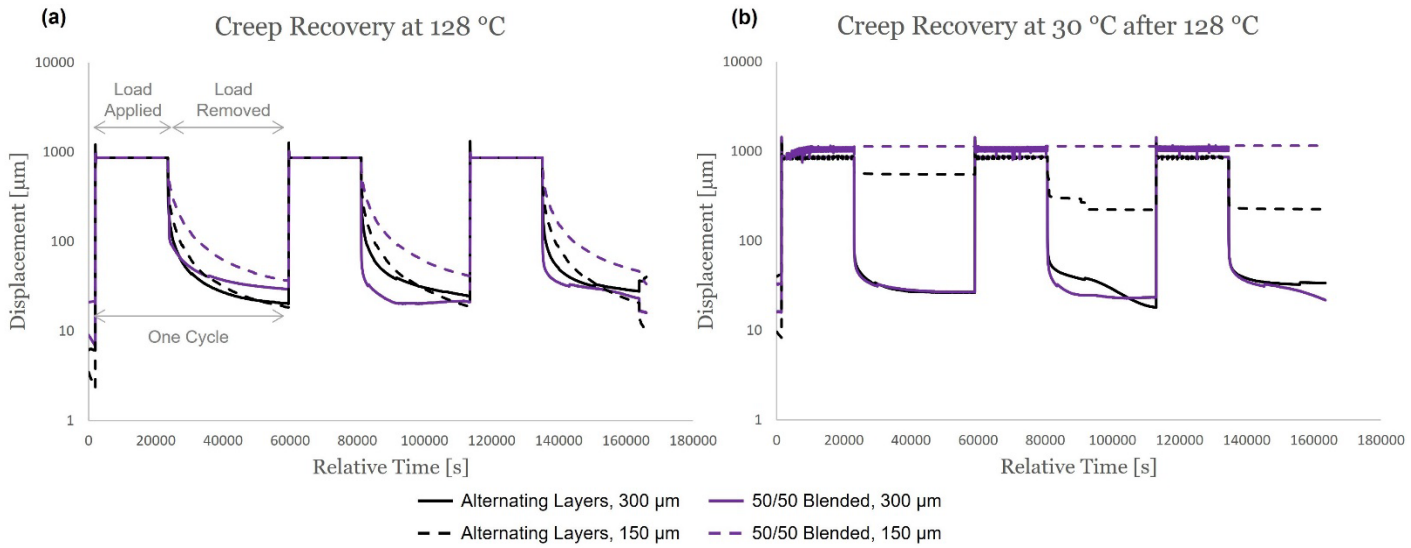

Figure 5: Comparison of creep recovery at (a) 128 °C and (b) 30 °C for samples printed from 50/50 blended filament (purple) and alternating homopolymer layers (black). Solid lines represent samples printed with 300 μm layer height and dashed lines represent samples printed with 150 μm layer height.

Figure 5(b) reports creep recovery at room temperature following the creep recovery experiment at elevated temperature. Here, no meaningful difference is observed between the samples with 300 μm layer height; both exhibit full recovery within the testing window. However, full recovery is not observed for either sample printed at 150 μm layer height, although the sample with alternating homopolymer layers exhibits a greater extent of recovery. The flatline response after returning to room temperature for the 50/50 blended samples printed at 150 μm likely indicates permanent deformation akin to compression set in foams. A comparison against PS and PC printed homopolymer samples will be included as future work.

Summary and Future Work

The presented work explores the unique opportunity afforded by fused filament fabrication (FFF) additive manufacturing (AM) to spatially template a polymer blend in a periodic manner. These samples comprising "alternating homopolymer layers" were compared against the traditional method for preparing polymer blend (i.e., melt-mixing in a twin screw extruder), and the pure polystyrene (PS) and polycarbonate (PC) homopolymer controls. The thermomechanical response of FFF printed samples was measured by dynamic mechanical analysis (DMA) in both oscillatory shear and creep modes in addition to differential scanning calorimetry (DSC). Glass transition behavior evaluation revealed distinct departure from the expected behavior for a miscible blend based on the Fox equation, thus indicating immiscibility. Trends in DMA behavior interestingly revealed that the sample of alternating 150 μm layers behaved more similar to the PC homopolymer instead of more similar to the traditionally melt-mixed blend. This deviation opens new possibilities for using AM to tailor material performance properties.

The difference in response between the samples under creep conditions compared with the trends observed for oscillatory shear conditions demonstrates the importance of evaluating the behavior of AM parts under a variety of load conditions. There have been other discussions in the

literature and broader community concerning the applicability of the ASTM dogbone shape for evaluating AM parts. It is likewise important to investigate how layered objects respond to varied load conditions. Polymer chain alignment plays a large role in interfacial behavior and is difficult to erase.

Future work should include a more detailed morphology to look at the dispersion of PC and PS in the blended filament. This may be done through either electron microscopy or Raman microscopy. Creep data should be collected for printed versions of PC and PS homopolymers. The presented work was able to compare the difference between two methods of preparation for nominally equivalent material compositions, however, a better interpretation can be made in the context of the homopolymer behavior.

The differences observed in the presented results arising from AM-tailored distribution of polymers inside a (macro-scale) blended morphology raise questions regarding how layerwise deposition can be exploited towards functionally graded materials or else realizing performance properties not possible to achieve through conventional methods of manufacturing. Since AM is fundamentally a technology reliant on sequentially mating and integrating surfaces, techniques prevalent in adhesion and surface sciences should be considered for increasing understanding of structure-process-morphology-performance relationships. Conversely, AM can be used as a tool to increase our understanding of surface science since whatever occurs at the layer-to-layer surface is magnified by the number of interfaces and periodicity of interfaces (i.e., layer height) in a part. Such an interdisciplinary pull and push between these two fields will vastly expand our knowledge and increase utility of AM as a viable means for end-use, performance-critical parts.

Acknowledgements

The authors thank Andrew Rhodes who supported sample fabrication and data collection. Blend preparation in the twin-screw extruder was performed by Justin Anderson through Mike Bortner's Polymer and Composite Manufacturing Laboratory at Virginia Tech.

This work was produced by Battelle Savannah River Alliance, LLC under contract number 89303321CEM000080 with the U.S. Department of Energy. Publisher acknowledges the U.S. Government license to provide public access under the DOE Public Access Plan (http://energy.gov/downloads/doe-public-access-plan). Direct funding was provided through the SRNL Laboratory Directed Research and Development (LDRD) program.

References

(1) Budhe, S.; Banea, M.; de Barros, S.; da Silva, L. An updated review of adhesively bonded joints in composite materials. *International Journal of Adhesion and Adhesives* **2017**, *72*, 30–42.

(2) Ultimaker, Ultimaker S3. 2021-2023; https://ultimaker.com/3d-printers/ultimaker-s3.

(3) Watschke, H.; Waalkes, L.; Schumacher, C.; Vietor, T. Development of novel test specimens for characterization of multi-material parts manufactured by material extrusion. *Applied Sciences* **2018**, *8*, 1220.

(4) Yin, J.; Lu, C.; Fu, J.; Huang, Y.; Zheng, Y. Interfacial bonding during multi-material fused deposition modeling (FDM) process due to inter-molecular diffusion. *Materials & Design* **2018**, *150*, 104–112.

(5) Freund, R.; Watschke, H.; Heubach, J.; Vietor, T. Determination of influencing factors on interface strength of additively manufactured multi-material parts by material extrusion. *Applied Sciences* **2019**, *9*, 1782.

(6) Lu, B.; Zhang, H.; Maazouz, A.; Lamnawar, K. Interfacial phenomena in multi-micro-/nanolayered polymer coextrusion: A review of fundamental and engineering aspects. *Polymers* **2021**, *13*, 417.

(7) Ponting, M.; Hiltner, A.; Baer, E. Polymer nanostructures by forced assembly: process, structure, and properties. Macromolecular symposia. 2010; pp 19–32.

(8) Painter, P. C.; Coleman, M. M. *Essentials of polymer science and engineering*; DEStech Publications, Inc, 2008.

(9) Kim, W. N.; Burns, C. M. Thermal behavior, morphology, and the determination of the Flory–Huggins interaction parameter of polycarbonate–polystyrene blends. *Journal of applied polymer science* **1987**, *34*, 945–967.

(10) Chevallier, C.; Becquart, F.; Taha, M. Polystyrene/polycarbonate blends compatibilization: Morphology, rheological and mechanical properties. *Materials Chemistry and Physics* **2013**, *139*, 616–622.

(11) Tanaka, Y.; Sako, T.; Hiraoka, T.; Yamaguchi, M.; Yamaguchi, M. Effect of morphology on shear viscosity for binary blends of polycarbonate and polystyrene. *Journal of Applied Polymer Science* **2020**, *137*, 49516.

(12) Ayoub, A.; Massardier-Nageotte, V. The effect of UV-irradiation and molten medium on the mechanical and thermal properties of polystyrene–polycarbonate blends. *Journal of Applied Polymer Science* **2012**, *124*, 1096–1105.

(13) Pal, R.; Sikder, A. K.; Saito, K.; Funston, A. M.; Bellare, J. R. Study of polycarbonate–polystyrene interfaces using scanning transmission electron microscopy spectrum imaging (STEM-SI). *Polymer International* **2023**, *72*, 106–112.

(14) Charif, I.; Doulache, N.; Gourari, A.; Rodrigue, D.; Giroux, Y.; Cherfi, R. Physical aging of PC: PS blends: Dynamic mechanical analysis and nuclear magnetic resonance studies. *Polymer Engineering & Science* **2022**, *62*, 3450–3461.

(15) Lee, J. K.; Han, C. D. Evolution of polymer blend morphology during compounding in a twin-screw extruder. *Polymer* **2000**, *41*, 1799–1815.

(16) Frunzaverde, D.; Cojocaru, V.; Bacescu, N.; Ciubotariu, C.-R.; Miclosina, C.-O.; Turiac, R. R.; Marginean, G. The Influence of the Layer Height and the Filament Color on the Dimensional Accuracy and the Tensile Strength of FDM-Printed PLA Specimens. *Polymers* **2023**, *15*.

(17) Abbott, A.; Tandon, G.; Bradford, R.; Koerner, H.; Baur, J. Process-structure-property effects on ABS bond strength in fused filament fabrication. *Additive Manufacturing* **2018**, *19*, 29–38.